

Investigation of shear wave velocity depth variability, site classification, and liquefaction vulnerability identification using near-surface V_s model of Christchurch, New Zealand

Christopher R. McGann*, Brendon A. Bradley, Misko Cubrinovski

Department of Civil and Natural Resources Engineering, University of Canterbury, Private Bag 4800, Christchurch, New Zealand

ARTICLE INFO

Keywords:

Cone penetration test (CPT)
Shear wave velocity
Liquefaction
Site classification

ABSTRACT

Following the companion work of McGann et al. [1], several applications of a regional surficial shear wave velocity (V_s) model developed for Christchurch, New Zealand are examined. Comparisons of time-averaged V_s over various profile depths are used to characterize the inherent depth variability of the soils in the region. The degree of correlation between 30 m shear wave velocity (V_{s30}) and average velocity over shallower profile depths (V_{sz}) exhibited by the current model is compared to similar correlations developed for other locations, and consideration is given to differences between the four primary surficial geologic units present in the majority of the Christchurch urban area. The effects of the observed V_s depth variability on expected seismic response are assessed through the consideration of transfer functions developed for 30 m typical V_s profiles for eight subregions of Christchurch. The regional V_s model is also used to develop site classification maps for Christchurch using current New Zealand and international site classification schemes, and these maps are used to comment on the applicability of these conventional schemes to the soil profiles typical to the region. Models of 5 m shear wave velocity (V_{s5}) filtered by average soil behaviour type index are used to examine the relationship between V_{s5} and observations of liquefaction-related surface damage made following the 22 February 2011 Christchurch earthquake. It is shown that when properly filtered to remove regions with soils that are less susceptible (or not susceptible) to liquefaction due to soil composition, there is a good correlation between V_{s5} and severity of liquefaction-related damage.

1. Introduction

The 4 September 2010 M_w 7.1 Darfield and 22 February 2011 M_w 6.2 Christchurch earthquakes resulted in strong ground motions throughout the greater Christchurch urban area [2,3]. The Darfield earthquake occurred about 15 km west of central Christchurch city, and resulted in moderate damage to local infrastructure and widespread liquefaction [4,5], while the Christchurch earthquake occurred approximately 4 km southwest of the city center, and the high-frequency amplitudes of the resulting ground motions across most of the city were much larger than in the Darfield event [2,3]. Liquefaction and lateral spreading associated with the Christchurch earthquake were significantly more severe and widespread than was observed the previous September, and accounted for the majority of the severe damage to properties and infrastructure [6–9].

The significant spatial variability of surficial ground motions

recorded from these two strong earthquakes, among others, illustrates the importance of local site effects (seismic response of surficial soils) on surface ground motion and the importance of site-specific response analysis. The response spectra for the Darfield and Christchurch events were similar at multiple Christchurch strong motion stations despite the clear differences in source and path effects [10,11], though this was not observed at all stations. For example, several strong motion stations were located in areas where liquefaction was prevalent during the 22 February event, but not observed in the 10 September earthquake. The increased amplitudes characteristic of the Christchurch earthquake resulted in larger shear deformation and associated excess pore pressure build-up compared to the Darfield event, and the occurrence of liquefaction-related phenomena was correspondingly more significant and widespread. The resulting differences in the recorded ground motions at these stations provide further evidence for the importance of site-specific analysis [10], and further support the need for a detailed characterization of the spatial and depth variability

* Corresponding author.

E-mail addresses: christopher.mcgann@canterbury.ac.nz (C.R. McGann), brendon.bradley@canterbury.ac.nz (B.A. Bradley), misko.cubrinovski@canterbury.ac.nz (M. Cubrinovski).

<http://dx.doi.org/10.1016/j.soildyn.2016.10.025>

Received 10 June 2015; Received in revised form 17 August 2016; Accepted 17 October 2016

Available online 23 November 2016

0267-7261/ © 2016 Elsevier Ltd. All rights reserved.

of soils in the near-surface (depth <30 m) zone, particularly over the range of depths where liquefaction-related phenomena most often occur.

Design and building codes in New Zealand and internationally typically provide a site classification system with which to group soil deposits with continuously-varying, and often highly variable, strength and stiffness properties into a series of discrete categories. Such site classification systems inherently assume that it is acceptable for design purposes to account for local site effects in an approximate manner in lieu of site-specific characterization, and each site class provides distinct seismic design considerations based on the general expected soil response represented by the chosen classification system to be used as guidance in the design of structures. Travel time-averaged shear wave velocity to 30 m depth (V_{s30}) is the primary site classification metric currently used internationally; in the United States via the National Earthquake Hazards Reduction Program (NEHRP) [12,13] site classes, and in Europe via Eurocode 8 [14]. In New Zealand, the seismic design specifications contained in NZS1170.5:2004 [15] prescribe site classification based primarily on the small-strain site period, taken as four times the estimated or measured travel time of shear waves from the surface to underlying rock, with the soil-to-rock transition defined by a compressive strength ≥ 1 MPa. While such discrete site classification systems tend to oversimplify the importance of local site effects and site-specific response analysis, they are valuable in the sense that they can give an overall picture of regional variability in expected seismic response.

In this paper, the near-surface V_s model of Christchurch, New Zealand developed using the methodology discussed by McGann et al. [1] is used to characterize and investigate the inherent subsurface variability of the region in several ways. Firstly, the variability in V_s with depth across the region is examined via comparison of time-averaged shear wave velocity for various profile depths (V_{sz}). In particular, the relationship between V_{s30} and V_{sz} values for profiles depths $z < 30$ m for the Christchurch soils is compared to similar relationships observed for sites in California [16], Japan [17], and Greece [18]. Secondly, transfer functions for typical 30 m V_s profiles at eight Christchurch subregions were computed to characterize the variation in expected small-strain seismic response due to the inherent depth variability. Site classification maps were also developed for the region using the site classification schemes prescribed by NZS1170.5:2004 [15] and NEHRP [12,13]. Thirdly, a regional model of 5 m time-averaged shear wave velocity (V_{s5}) is compared to the liquefaction-induced land damage map of van Ballegooy et al. [9] in order to determine if trends in the V_{s5} models correspond to the observed regional liquefaction vulnerability.

2. Regional V_{sz} models

Models of V_{sz} for $z=5, 10, 20$, and 30 m were developed over the Christchurch region using the procedure discussed by McGann et al. [1]. The regional V_{sz} models developed for the different target profile depths are useful for different purposes, with no one single model providing the means with which to fully characterize the expected seismic response of a particular site. The models for the shallower target depths, for example the regional V_{s5} (shown in Fig. 1) and V_{s10} (not shown here) models, can be used to provide a provide a characterization of the very-near-surface soils that can be useful in describing the regional distribution of soft and stiff soils within this zone. The models for the deeper target depths, in particular the V_{s30} model shown in Fig. 2 (reproduced from [1]), provide an indication of how a site may respond in an overall sense during earthquake shaking and how this expected overall response varies across the greater Christchurch area. The full set of regional models created for 5, 10, 20, and 30 m profile depths are available in McGann et al. [19] along with associated maps showing the distributions of V_{sz} at the CPT sites used in the development of each model.

These models reveal the significant spatial variability in V_s for the region, and through comparison of the V_{s5} and V_{s30} models, indicate a similar variability with respect to depth. Some features present in the V_{s30} model correspond directly to the V_{s5} model, such as the increased velocities for the marine/dune sands near the Pacific coast and for the over-bank gravel lobes [20] to the west where the profiles are consistently more stiff on average than the surrounding areas. For regions where the V_{sz} models have relatively contrasting values, the surfaces shown in Figs. 1 and 2 provide some insights into the profile characteristics and expected seismic responses. Profiles located in areas with lower V_{s5} may be relatively soft on average over the full 30 m in comparison to the entire region (e.g. Sydenham and Papanui, near boxed regions 4 and 5, respectively), or may be relatively stiff on average (e.g. Kaiapoi and parts of Halswell) due to changes in the soil profile occurring below 5 m depth.

2.1. Assessment of shear wave velocity depth variation

The degree of correlation between the various V_{sz} models is assessed by comparing the V_{s30} values at the grid points of the regional model with the corresponding V_{sz} values for profile depths $z < 30$ m. These comparisons are made separately for the grid points located in each of the four primary surficial geological units (QMAP units) considered in this study: alluvium, marine/dune, estuarine, and peat/swamp (see McGann et al. [1] for further information). Fig. 3 presents the results of the comparisons, and Table 1 provides the coefficients of determination, r^2 , and lognormal standard deviations, σ_e , between V_{sz} and V_{s30} for the full dataset (all QMAP units) and the sites within each QMAP unit. As shown in Fig. 3, the degree of correlation between V_{sz} and V_{s30} differs depending on the QMAP units of the Christchurch sites. For sites in the alluvial, marine/dune, and estuarine QMAP units that comprise the majority of the overall dataset, there is little correlation between V_{s5} and V_{s30} , and the degree of correlation between V_{sz} and V_{s30} generally increases with profile depth. A much stronger correlation is observed for all profile depths in the peat/swamp sites, especially relative to the other QMAP units. This increased correlation is likely due to the soil profiles of the peat/swamp sites, which are often characterized by relatively thick layers of low V_s soils near the ground surface that substantially affect, and tend to homogenize, V_{sz} values due to their prominence in the profiles. The differences in the degree of correlation between V_{s30} and V_{sz} in terms of the surficial geologic units highlights the importance of consideration for the one prevalent soil type or layer (low or high V_s) that controls the 30 m velocity profile when computing V_{s30} . The scatter evident in the results of Fig. 3 and Table 1 indicates that the use of mean-value empirical equations for this purpose should be done with care, especially for shallow depths.

The lack of correspondence between V_{s30} and V_{sz} for shallow z in the non-peat/swamp sites observed in Fig. 3 is inferred as a result of the stratified nature of the soils underlying the Christchurch region. The upper boundary of the Riccarton Gravel that underlies most of the region is <30 m below the ground surface [1,20,21]. For a given site, the shear wave velocity of the Riccarton Gravel is both independent of, and much larger than, that in the overlying soils, therefore, V_{sz} values for depths above the Riccarton Gravel will not directly correspond to velocities averaged over the entire 30 m profile. The relationship between the depth to the Riccarton Gravel and the degree of correlation between V_{sz} and V_{s30} is evident in the spread in the data points for the alluvium and marine/dune sites in the V_{s5} and V_{s10} plots of Fig. 3. The sites that plot nearer the 1:1 correlation line are likely those sites where the Riccarton Gravel is deep (i.e. eastern areas), and the sites that plot nearer the left-hand edge of the plots are likely those where the Riccarton Gravel is shallow (i.e. western areas and those near the Port Hills to the south). In effect, for the alluvium and marine/dune sites, moving from left to right across the data points (for a given y -axis value) in the V_{s5} subplot of Fig. 3 represents a move from west to east across Christchurch.

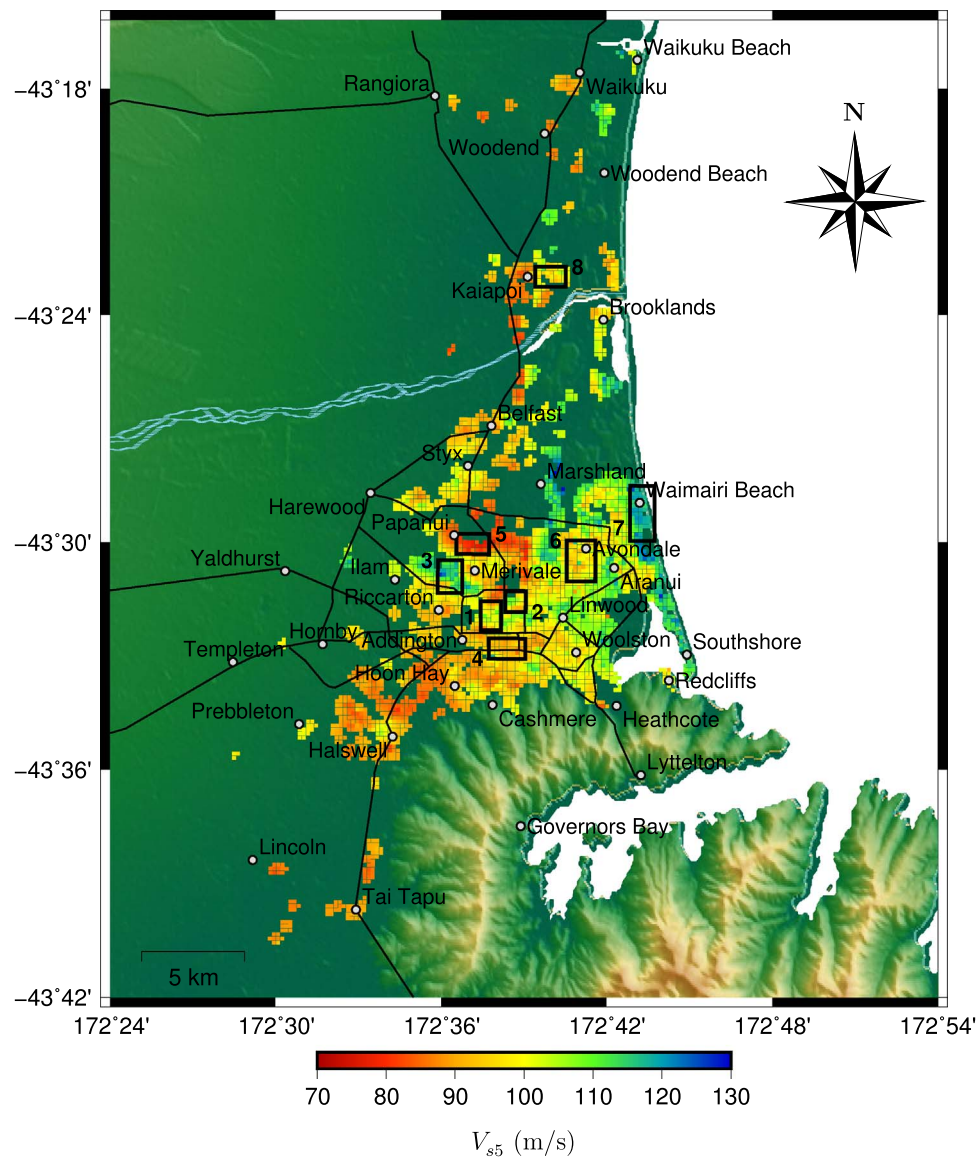


Fig. 1. V_{s5} surface on uniform 200×200 m grid. Predictions are only provided in each grid cell if there is one or more CPT record within 300 m. Numbered boxes refer to subsequently discussed subregions of specific interest.

2.2. Comparison to existing V_{sz} - V_{s30} prediction models

The V_{s30} values estimated by three V_{sz} prediction models [16–18] are added to Fig. 3 for reference. The dot-dashed lines show the results for the Boore [16] model developed using V_s profile data from strong-motion stations in California (model not applicable to V_{s5}), the dashed lines show the results for the Boore et al. [17] model developed using V_s profile data from boreholes at Kiban-Kyoshin Network (KiK-net) stations in Japan, and the dotted lines show the results for the Stewart et al. [18] model developed using V_s profile data from various sites in Greece. As shown, these three external datasets describe quite different relationships between V_{sz} and V_{s30} , particularly for shallower profile depths, where the inherent variability of the soil is most impactful. The Japan-based model tends to estimate the highest V_{s30} values for a given value of V_{sz} and appears to be the most representative of the Christchurch data. The California-based model tends to estimate the lowest V_{s30} values for a given value of V_{sz} , and the Greek model estimates tend to be in between these extremes for the range of velocities shown here.

The differences between these models with respect to each other and with respect to the Christchurch data are likely due to the composition of the soil profiles and soil types represented by the datasets. The California stations were primarily sited in the Los Angeles and San Francisco areas, which are typically underlain by sedimentary basins that are relatively uniform in nature in the first 30 m below the ground surface [17]; subsurface conditions not representative of those in Christchurch. In contrast, the KiK-net sites are from locations throughout the entire Honshu region of Japan and thus represent a larger variety of soil conditions; specifically including areas of shallow sediment over rock [22] that are more similar in nature to the conditions in Christchurch. The Greek sites are similarly representative of a wider variety of subsurface conditions, but it is likely that a lack of sites with shallow sediments over rock or dense sand/gravel leads to the lower V_{s30} values evident in Fig. 3 and the corresponding lack of applicability to the Christchurch data. Overall, the differences between the V_{s30} values for these four global datasets indicates the importance for site-specific measurements of shear wave velocity when possible, and for region-specific estimation techniques when site-specific mea-

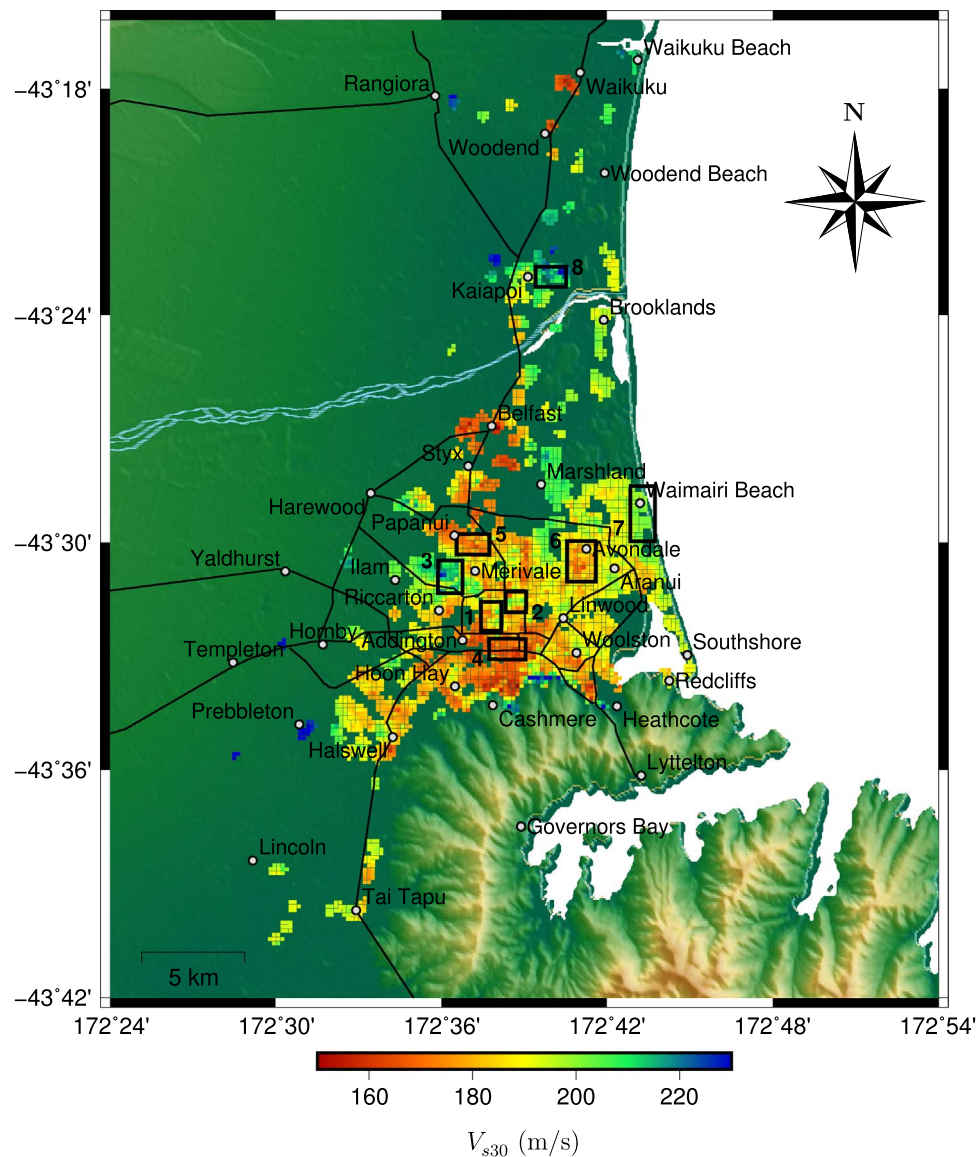


Fig. 2. V_{s30} surface on uniform 200×200 m grid (after [1]). Predictions are only provided in each grid cell if there is one or more CPT record within 300 m. Numbered boxes refer to subsequently discussed subregions of specific interest.

measurements are not available.

3. Site classification from regional V_{sz} models

Seismic design guidelines and codes commonly designate site soil classification systems to dictate various design requirements for structures located on different general site types (e.g., soft soil, stiff soil). These site classification systems are often based at least partially on shear wave velocity data, thus, the regional V_{sz} models are particularly well suited to the development of such site classification maps for the Christchurch area. NEHRP [12,13] defines site classes based on V_{s30} (with the exception of site class F for special conditions), and is the standard system used in the United States. In New Zealand, NZS1170.5 [15] defines site classes based on several factors, including V_{s30} , small-strain natural period of soil above bedrock, and the thickness of soft soil (as defined by $V_s < 150$ m/s) within a given profile. The Christchurch V_{sz} models are used to develop site classification maps under each system both to characterize the site classes present in the region and to highlight the similarities and differences of the NEHRP and NZS1170.5 systems. For reference, the NEHRP and

NZS1170.5 site classification systems are summarized in Appendix A.

Fig. 4 shows the NEHRP site classes based on the V_{s30} model of Fig. 2 (without regard for the special conditions of site class F). The Christchurch sites considered in this research are characterized as either NEHRP site class D (blue markers, $180 < V_{s30} \leq 360$ m/s) or class E (red markers, $V_{s30} \leq 180$ m/s). The class E sites primarily correspond to known areas of silty, clayey, or swampy soils such as Papanui and Sydenham [23,24]. There are also a few sporadic zones of class E soils along the path of the Avon river through the eastern suburbs of the city where loose sandy soils are present near the surface and silty and clayey soil types are present at greater depths [1]. Because only those CPT sites that penetrated to a useful depth were used, and because sites in loess deposits were omitted due to non-applicability of the Christchurch-specific CPT- V_s model of McGann et al. [25,26] to this soil type, the results of Fig. 4 do not depict stiff sites in western Christchurch or the Port Hills which may potentially be characterized as NEHRP site classes B or C. Fig. 4 also shows the distribution of V_{s30} within each NEHRP site class, with the solid black lines denoting the mean V_{s30} for the distribution corresponding to each class. As shown, the majority of the class D sites have $V_{s30} < 200$ m/s and increasing V_{s30}

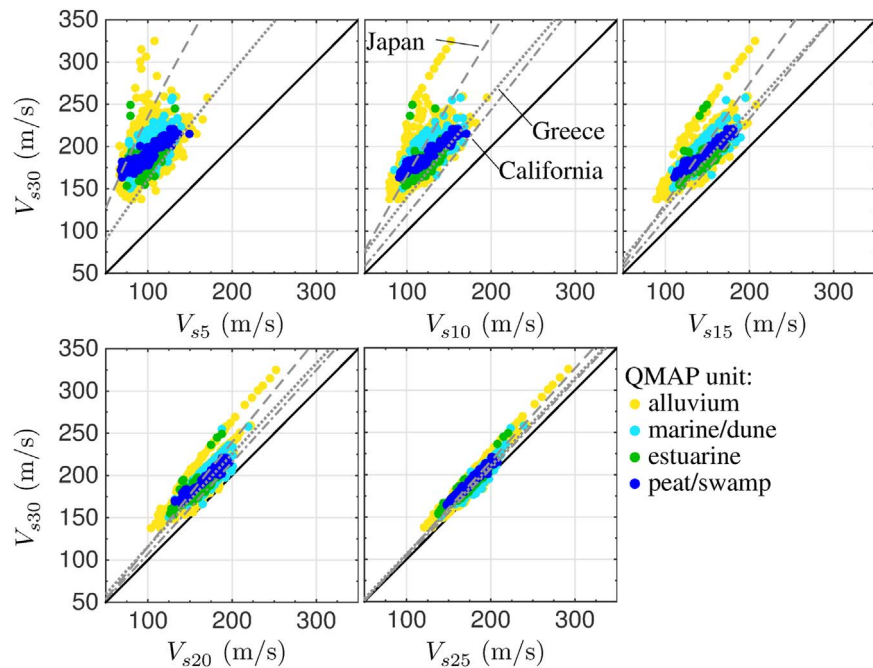


Fig. 3. Comparison of V_{sz} with V_{30} for $z = 5, 10, 15, 20, 25$ m. Marker colour indicates surficial QMAP geologic unit. Dot-dashed, dashed, and dotted lines indicate regression models of Boore [16], Boore et al. [17], and Stewart et al. [18], respectively (data not available at 5 m depth in [16]).

is associated with decreasing frequency of occurrence. Similarly, the bulk of the class E sites are concentrated near the $V_{30} = 180$ m/s boundary and there are relatively few locations with $V_{30} < 165$ m/s. Due to the $200\text{ m} \times 200\text{ m}$ grid adopted during the creation of the V_{30} model [1], there may be isolated areas within these grid spaces that have lower or higher V_{30} values than the ranges shown here.

Fig. 5 shows the NZS1170.5 site classes determined from the regional shear wave velocity models. In contrast to the NEHRP classification system, the NZS1170.5 site classes are not based solely on V_{30} , therefore, the development of the site classes shown in Fig. 5 required some additional steps. Because the V_{30} model does not include any locations with $V_{30} > 360$ m/s, site classification for this model under the NZS1170.5 scheme need only consider classes C, D, and E (shallow soil sites, deep/soft soil sites, and very soft soil sites, respectively). The designation between class C and D sites was made with respect to the small-strain site period of the soils above the rock (T_{soil}). Site periods were computed as 4 times the V_s travel time through all non-rock strata, and those locations with $T_{\text{soil}} < 0.6$ seconds were assigned site class C. Due to the nature of the stratigraphy beneath the Canterbury plains, where the basement rock is quite deep and site periods are generally large [27], the class C sites are confined to the vicinity of the Port Hills where the underlying volcanic rock is relatively shallow. The classification for site class E was made by creating a regional model of soft soil profile thickness (as defined by $V_s < 150$ m/s)

from the CPT-based V_s in a manner similar to that used to create the V_{sz} models. The class E sites shown in Fig. 5 are those locations where the depth of soft soils is ≥ 10 m.

The distributions of V_{30} within each NZS1170.5 site class are also shown in Fig. 5, with the solid black lines denoting the mean of the distribution for each site class. Note that the scales on the vertical axes are not the same for each case. These V_{30} distributions show that while there is a general correlation between NZS1170.5 site class and the mean V_{30} for each class, there is little correlation in an overall sense (i.e. a particular value of V_{30} does not necessarily correspond to any particular site class). There is a distinct tendency for NZS1170.5 class E sites to have $V_{30} < 180$ m/s, as 10 m of soil with $V_s < 150$ m/s drives down the 30 m average value, however, there are actually more class D grid points in this velocity range than total class E grid points. Similarly, the because the distinction between site classes C and D is made primarily on the basis of site period for soils above rock, these site classes provide no real information for the velocities of the non-rock strata or even necessarily any information about expected seismic response. For example, the surficial seismic response for a western Christchurch site where the Riccarton Gravel interface is at 15 m depth would be expected to be quite different than at an eastern Christchurch site where this interface is >30 m depth, however, both sites are classified as NZS1170.5 class D, and the design response spectra would be the same. This idea is explored further in the following section using

Table 1
Coefficients of determination, r^2 , and lognormal standard deviations, σ_e , between V_{sz} and V_{30} for QMAP units and overall dataset.

QMAP Unit	V_{s5}		V_{s10}		V_{s15}		V_{s20}		V_{s25}	
	r^2	σ_e	r^2	σ_e	r^2	σ_e	r^2	σ_e	r^2	σ_e
Alluvium	0.35	0.069	0.47	0.062	0.59	0.055	0.76	0.043	0.93	0.024
Marine/dune	0.45	0.033	0.58	0.028	0.69	0.024	0.77	0.021	0.86	0.017
Estuarine	0.34	0.047	0.46	0.043	0.60	0.037	0.76	0.029	0.92	0.017
Peat/swamp	0.83	0.033	0.91	0.024	0.95	0.019	0.94	0.018	0.96	0.016
All data	0.43	0.057	0.53	0.051	0.65	0.045	0.78	0.036	0.91	0.023

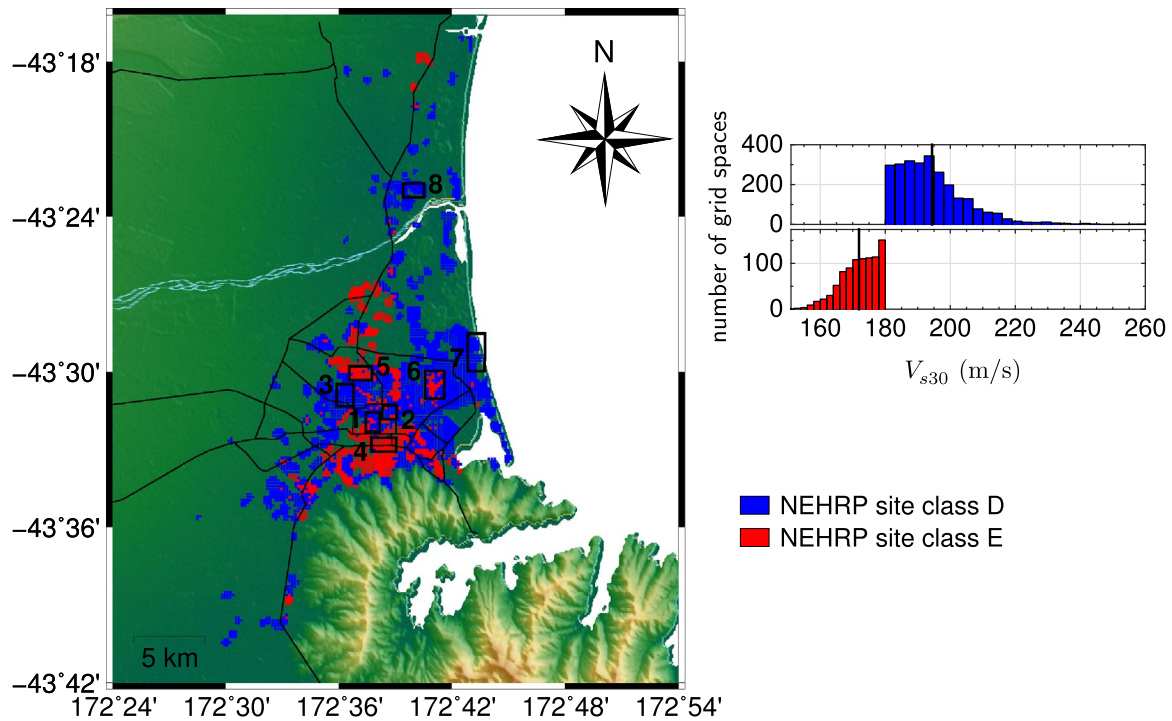


Fig. 4. NEHRP site classes [12,13] from Christchurch V_{s30} model and distribution of V_{s30} within each class. Site class F is ignored. Numbered boxes refer to subsequently discussed regions of specific interest.

typical 30 m profiles for eight Christchurch subregions.

A comparison of Figs. 4 and 5 shows that the primary differences between the two site classification schemes concern the NZS1170.5 class C sites, which are not represented by the NEHRP classification system, and the regions classified as soft soil sites (class E in both cases). As shown, there is not a 1:1 correspondence between the soft soils definitions for the NEHRP and NZS1170.5 classification systems.

In general, areas designated class E under NZS1170.5 are also designated as class E by the NEHRP system, however, the opposite observation does not hold as many locations with $V_{s30} < 180$ m/s do not have profiles with $V_s < 150$ m/s for 10 m or more and fall under NZS1170.5 site class D instead. Based on the soft soil depth model generated to determine the NZS1170.5 class E sites, as the required soft soil thickness is decreased from 10 m, there is an increasing

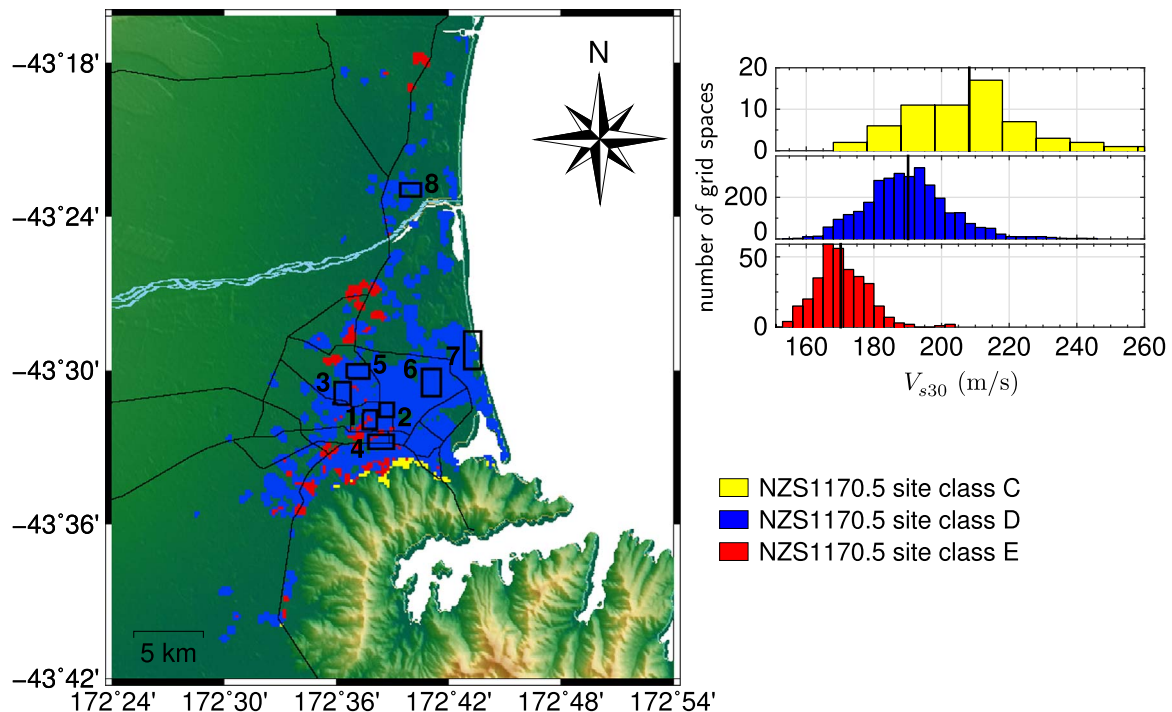


Fig. 5. NZS1170.5 site classes [15] from Christchurch V_{s30} models and distribution of V_{s30} within each site class. Numbered boxes refer to subsequently discussed regions of specific interest.

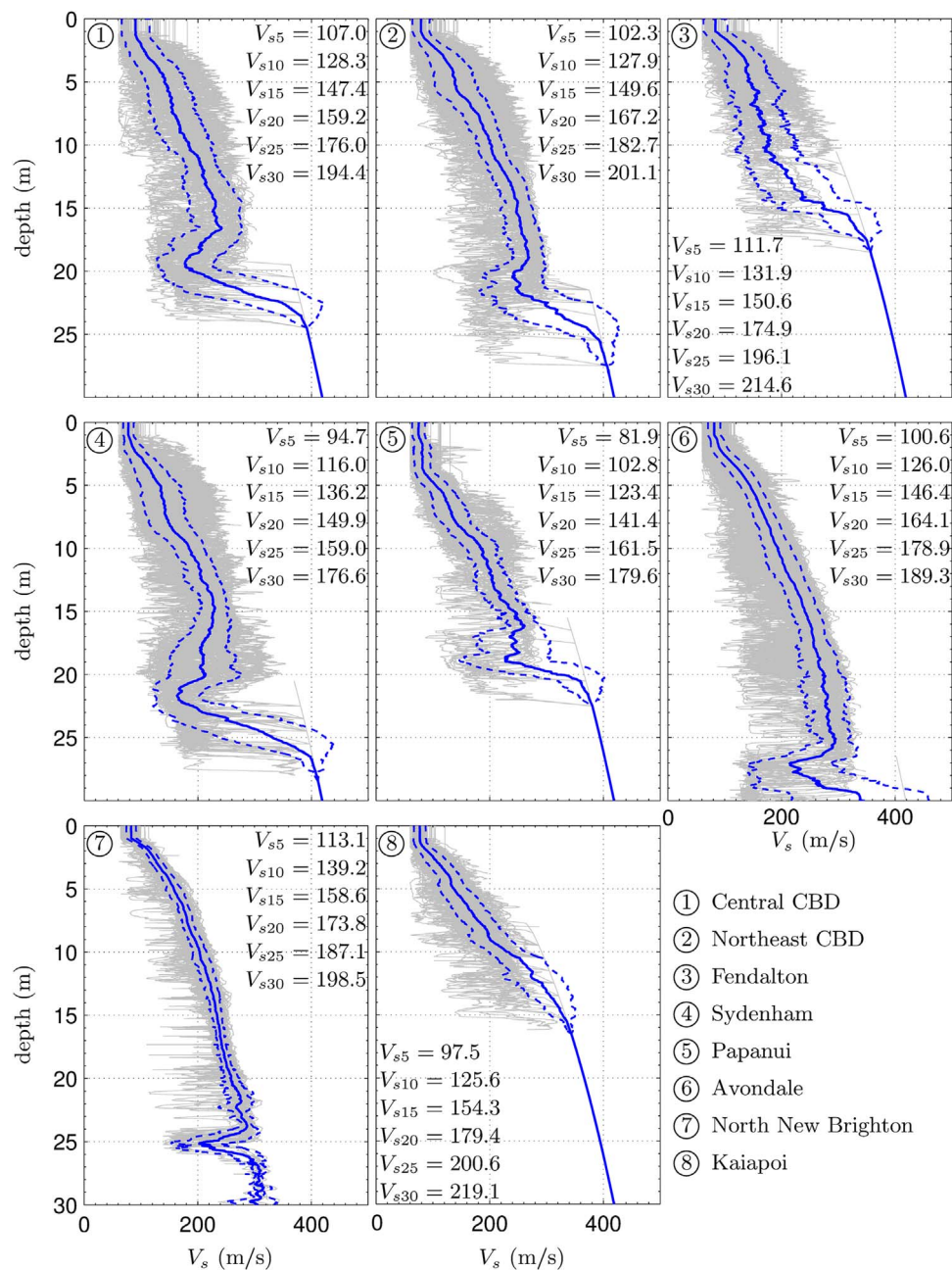


Fig. 6. Typical V_s profiles for 8 Christchurch subregions including estimated gravel velocities for depths below top of Riccarton Gravel surface. Region number is noted in upper left of each plot.

correspondence between the regions designated as class E by the NEHRP and NZS1170.5 schemes, though a 1:1 correspondence does not exist for any soft soil thickness due to the differences in classification method.

4. Small-strain seismic response of typical 30 m V_s profiles

The V_{s5} and V_{s30} models of Figs. 1 and 2 reveal the inherent variability of the regional soil profiles in the sense of both depth and spatial location, and give an overall picture of the relative V_s values of different areas, but cannot be directly used to assess how these differences may affect the expected surficial response to a given ground motion. The typical V_s and soil behaviour type index (I_c) profiles developed for eight subregions throughout Christchurch in McGann et al. [1] are used for this purpose through the computation of transfer functions for the mean 30 m V_s profiles applicable to each subregion.

As shown in Figs. 1, 2, 4, and 5, these subregions are located across the Christchurch region and are representative of a variety of V_{s5} and V_{s30} values and site classes. Comparisons of the transfer functions for the V_s profiles typical to these subregions therefore aids in identifying how the inherent depth variability of the soils throughout the Christchurch region may lead to different site-specific responses, and how different subregions differ from each other.

4.1. Characterization of typical profiles to 30 m depth

The typical V_s profiles obtained for the considered subregions and presented in McGann et al. [1] provide a description of the soil shear wave velocities for all depths with at least one CPT record. To characterize these profiles up to a depth of 30 m, an estimated Riccarton Gravel surface [21,28] (see McGann et al. [1] for more information on the background and scope of this surface) is used to

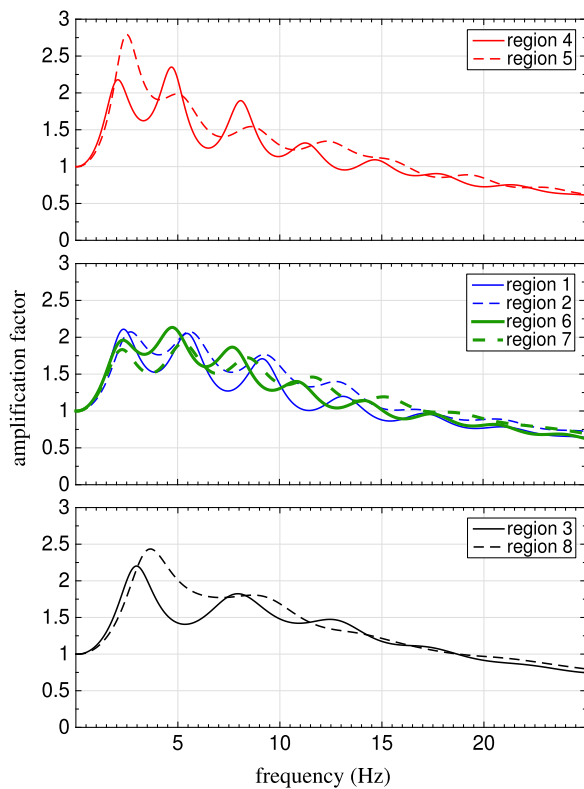


Fig. 7. Transfer functions for 8 Christchurch subregions grouped by V_{s30} .

determine the depth to the Riccarton Gravel at each CPT site. Assumed velocity profiles for the Riccarton Gravel are computed using Eq. (3) of McGann et al. [1] and appended to the appropriate depths. The 30 m V_s profiles for all 8 subregions are shown in Fig. 6 along with V_{sz} values determined on 5 m intervals from each modified mean V_s profile (no uncertainty is considered in the estimated Riccarton Gravel velocity profiles). The solid and dashed blue lines in Fig. 6 represent the mean and \pm standard deviation V_s profiles, and the thin gray lines represent the V_s profiles obtained from all of the CPT logs in each subregion. The fill-in criteria discussed in McGann et al. [1] is not considered in the computation of these typical 30 m profiles. The typical V_s profiles above the Riccarton Gravel are informed only by recorded data.

In an overall sense, the V_{s30} values for all of the subregions are all similar, having a range of 177–219 m/s. This overall similarity also holds in the context of the NEHRP [12,13] and NZS1170.5 [15] site classification systems. Per Fig. 4, regions 3, 7, and 8 are entirely composed of NEHRP site class D soils, regions 4 and 5 are essentially entirely composed of site class E, and regions 1 and 2 contain a mix of site class D and E locations. Based on the V_{s30} values of the typical 30 m profiles shown in Fig. 6, only regions 4 and 5 are NEHRP class E profiles. The remaining regions all meet the class D criteria. In terms of the NZS1170.5 site classes shown in Fig. 5, all eight subregions are primarily, if not entirely, composed of NZS1170.5 site class D soils. Only regions 1 and 4 contain any locations meeting the criteria for site class E. Despite this nominal similarity in V_{s30} and site classification, Fig. 6 shows that there is a fair amount of variability in the typical V_s profiles for the considered subregions both in terms of the shear wave velocities over different depth intervals, and in terms of the depth to the top of the Riccarton Gravel. The inclusion of the Riccarton Gravel velocity profiles results in a slight increase in the deepest non-gravel V_{sz} values (e.g., in region 2, $V_{s25} = 176.1$ m/s without gravel velocity and 182.7 m/s with the gravel velocity), as the presence of the Riccarton Gravel at these depths naturally drives up the average shear wave velocities.

4.2. Transfer functions for typical 30 m profiles

Transfer functions are computed from the mean V_s profiles shown in Fig. 6 to investigate the similarities and differences in small-strain seismic response for 30 m deep profiles within the considered Christchurch subregions. As shown in Fig. 6, several of the subregions with dissimilar V_s profiles are similar in terms of V_{s30} (e.g., regions 4 and 5), and it is of interest to assess to what degree that these differences in soil profile are manifested as differences in surficial site response. Because the transfer functions are based on the assumption of linear response, it is not expected that any observations made here will necessarily hold for large amplitude ground motions that induce nonlinear soil behaviour. Factors that are not captured here, such as soil composition, the relative distribution of soil density within the profile, and the location of the groundwater table become more important under large amplitude shaking and will arguably lead to further differences between the seismic response characteristics of the different deposits. However, the transfer functions for these velocity profiles provide a simple means with which to evaluate V_{s30} as a predictive metric for site response in the Christchurch area.

Fig. 7 shows the computed transfer functions for each subregion in terms of the variation in amplification factor with frequency. These transfer functions were computed assuming constant density $\rho = 1.8$ Mg/m³ and constant damping ratio $\xi = 5\%$ throughout all profiles (because the transfer functions are only weakly dependent on these two parameters, which have little variation). Regions with similar V_{s30} values are grouped together in Fig. 7 to emphasize the relative differences in seismic response indicated for regions that are classified as similar according to V_{s30} -based criteria such as the NEHRP site classes. The upper plot of Fig. 7 shows the soft subregions, Sydenham (region 4) and Papanui (region 5) where $V_{s30} < 180$ m/s; the middle plot includes the intermediate V_{s30} subregions, Avondale (region 6), North New Brighton (region 7), and the two central business district (CBD) regions (regions 1 and 2); and the lower plot shows the two stiff subregions, Fendalton (region 3) and Kaiapoi (region 8) where $V_{s30} > 210$ m/s due primarily to the presence of the shallow gravels discussed in McGann et al. [1]. As shown in Fig. 7, there are notable differences between the computed transfer functions for these typical profiles, and these differences are most apparent in the upper and lower plots of Fig. 7, which compare the transfer functions for the softest and stiffest regions, respectively.

The typical profiles for regions 4 and 5 have essentially identical V_{s30} values (176.6 and 179.6 m/s, respectively). However, based on the results of Fig. 7, given identical input motions at 30 m depth, the resulting surficial motions, and the associated effects on structural response, would likely be different. The peak amplifications occur at different frequencies (max amplification for region 4 at 4.7 Hz and at 2.5 Hz for region 5), occur in different vibration modes (mode 2 for region 4 and mode 1 in region 5), and have different amplitudes (max amplification factor is 2.4 in region 4 and 2.8 in region 5). In addition, higher mode effects are more prevalent for the region 4 profile than is observed for region 5, which is mostly first-mode dominant.

The typical profiles for regions 3 and 8 are also nominally identical in terms of V_{s30} (214.6 and 219.1 m/s, respectively) and display somewhat similar differences as observed in regions 4 and 5, though these differences are more subtle for these stiff profiles. The transfer functions for regions 3 and 8 have different peak amplification magnitudes (2.2 in region 3, 2.5 in region 8), and though both show first mode dominant responses, the peak amplifications occur in different frequencies (2.8 Hz in region 3, 3.7 Hz in region 8). The higher modes are also more prevalent in the transfer function for region 3 (i.e., higher modes are more distinct and amplification factors for higher modes are greater than or equal to those in region 8).

The transfer functions for the subregions shown in the middle plot of Fig. 7 (regions 1, 2, 6, and 7) are more similar to each other than in the previously discussed groupings, but differences are still apparent.

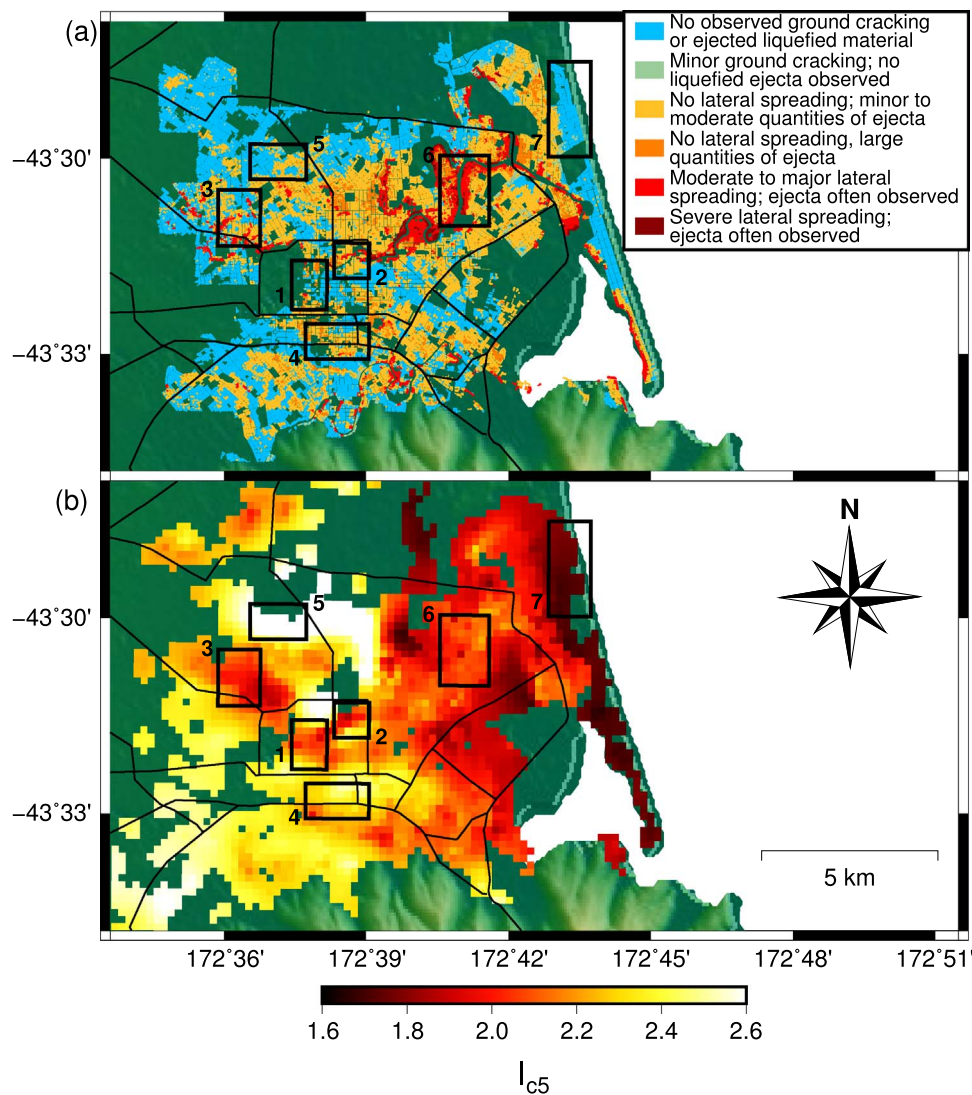


Fig. 8. Comparison of I_{c5} with observations of liquefaction severity following 22 February 2011 earthquake. (a) Liquefaction-induced land damage map after [9]; (b) I_{c5} surface. Numbered boxes refer to previously discussed subregions of specific interest.

The V_{s30} values for the profiles in all four of these subregions are within about 12 m/s of each other, however, there is a clear distinction between the transfer functions for the CBD (regions 1 and 2) and eastern Christchurch (regions 6 and 7) subregions that does not correspond to their relative V_{s30} values. The magnitude of the peak amplification in the first two modes of regions 1 and 2 are nominally identical at about 2.1, but the modal troughs in region 2 are less pronounced and the modal peaks are generally greater in amplitude beyond the second mode. For the eastern Christchurch subregions, the amplification and frequency for the first mode are similar (amplification of about 1.6–1.9 at 2.25 Hz) and the second mode response has a larger amplification factor in both cases. The higher modes in region 6 generally occur at lower frequencies than in region 7, and beyond the third mode, the amplification factors in the higher modes for region 7 are generally higher. In summary, it can be seen even with this simple metric that the explicit knowledge of V_s profiles available throughout the Christchurch region via this model can aid in better capturing site response variability and site-specific response than via the use of V_{s30} alone.

5. Regional V_{sz} model and liquefaction severity observations

The strong shaking associated with the events of the 2010–2011

Canterbury earthquake sequence triggered extensive liquefaction in the Christchurch area [5,8,9]. The residential liquefaction-induced land damage map in Fig. 8(a) presents observations made following the 22 February 2011 earthquake after van Ballegooy et al. [9]. The surface manifestations and damage associated with liquefaction were particularly severe in the suburbs to the east and immediate north of the CBD near the present-day route of the Avon river, and minor to moderate liquefaction-related damage was observed across much of Christchurch. The V_{s5} model shown in Fig. 1 corresponds reasonably well with the van Ballegooy et al. [9] liquefaction damage map, with areas where liquefaction occurred typically displaying lower V_{s5} values than areas where liquefaction was not observed (the implication being that lower V_s corresponds to lower relative density). For example, the boundary between the yellow and green markers ($V_{s5} \lesssim 105$ m/s) north-east of the CBD roughly approximates the boundary between severe and moderate damage shown in the corresponding region of Fig. 8(a), and the damage/no damage boundary near the coast is also clearly evident in the V_{s5} model. Despite such visual similarities in some regions of Christchurch, there are counter examples in other regions where low V_{s5} values do not correspond to any significant liquefaction damage, as soil composition and water table depth must also be considered.

The very soft locations indicated in Fig. 1 ($V_{s5} \lesssim 85$ m/s) are

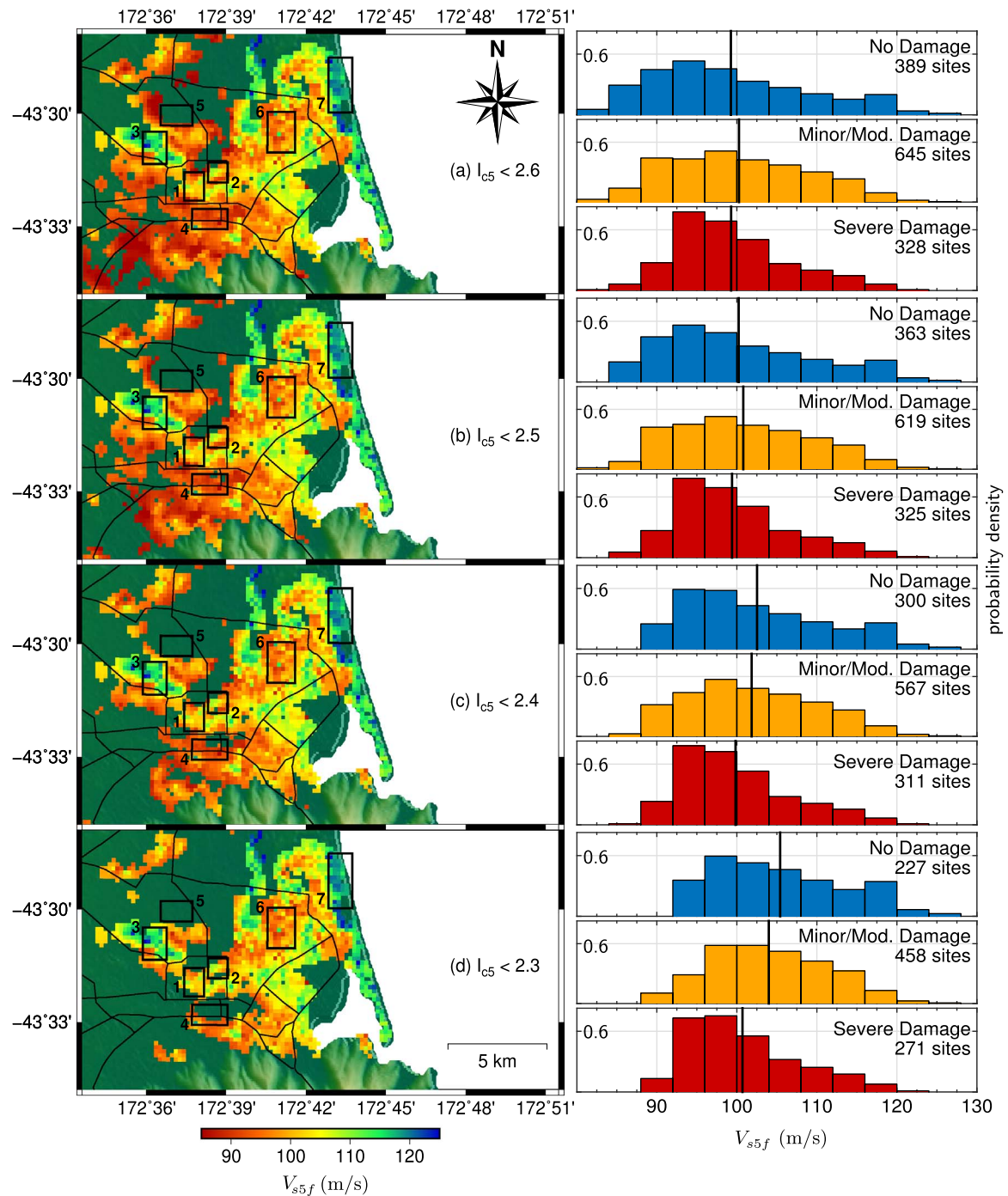


Fig. 9. V_{s5f} surfaces filtered by I_{c5} magnitude and distributions of liquefaction damage for model grid points. (a) $I_{c5} < 2.6$; (b) $I_{c5} < 2.5$; (c) $I_{c5} < 2.4$; (d) $I_{c5} < 2.3$. Numbered boxes refer to previously discussed subregions. Black lines in histograms indicate the mean V_{s5f} value for each damage category.

primarily areas where liquefaction did not occur or liquefaction-related surface damage was relatively minor. This is likely due to the nature of the soils in these regions. For example, in the soft zones located in the Papanui/Mairehau area north of the CBD and in the Sydenham area immediately south of the CBD, the soils in the upper 5–10 m are comprised primarily of silts, clays, and/or sands with high fines contents. While the predominance of these types of soils at shallow depths results in low values of V_{s5f} , these areas do not correspond to severe liquefaction observations as these types of soils are either less susceptible to liquefaction or not liquefiable (despite these regions

being susceptible to cyclic softening). These regions of low V_{s5f} values are highly correlated with locations of in-filled swamps, lagoons, and other wet areas as indicated in the 1856 black maps of Christchurch [24,29].

5.1. Consideration for soil composition

To remove the effects of such silty or clayey soils, and isolate the V_{sz} magnitudes corresponding to liquefaction-susceptible deposits, the average soil behaviour type index [30] within the uppermost 5 m of

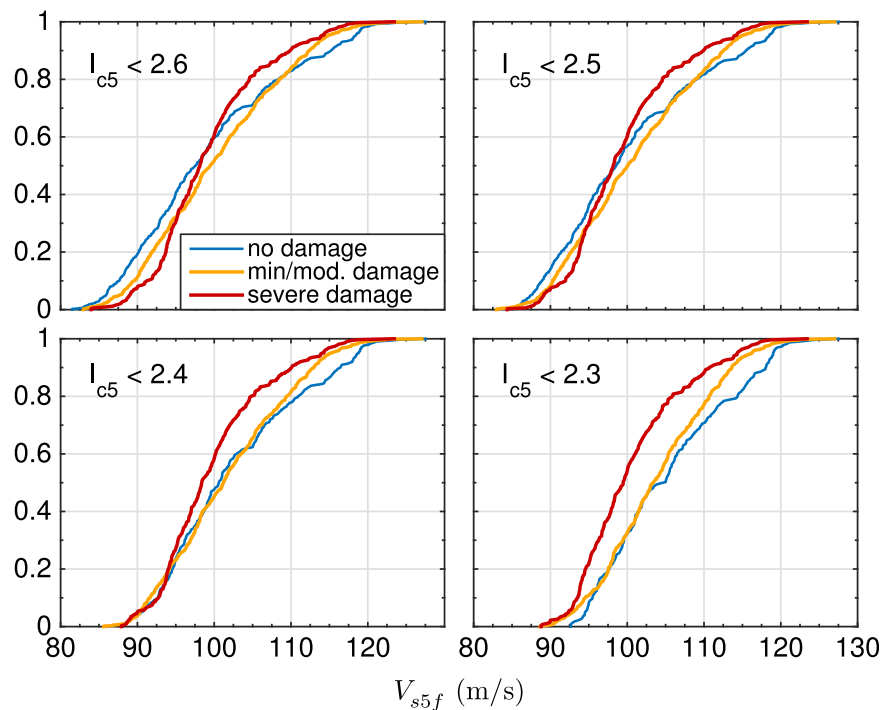


Fig. 10. Empirical cumulative distribution functions of V_{s5f} for three damage cases and four I_{c5} filters.

the ground surface is considered. This depth-weighted average index, I_{c5} , is computed as

$$I_{c5} = \frac{\sum (d_i I_{ci})}{\sum d_i} \quad (1)$$

where d_i are the depth increments over which each incremental I_{ci} value applies. The uppermost 1.2 m of soil is ignored in the determination of I_{c5} , as it is assumed that this crustal soil is not necessarily indicative of the soil types in the zone of interest and because there was often a pre-drill zone for most of the CPT soundings [1]. The I_{c5} model shown in Fig. 8(b) was developed in a manner similar to that for the V_{sz} models (model development described in McGann et al. [1]). Alternative I_{cz} values were considered (e.g., I_{c10}), however, a 5 m profile depth was selected to be consistent with the depth ranges considered in V_{s5} . As shown in Fig. 8, there is a general correspondence between areas of $I_{c5} > 2.3$ –2.4 and areas with less severe observations of liquefaction effects, while the areas where more severe liquefaction-related damage was observed tend to have lower I_{c5} values.

The V_{s5} values corresponding to the areas of more severe liquefaction-related damage are isolated by filtering out the areas where the shallow soils can be considered less susceptible to liquefaction or not liquefiable using bounding values of I_{c5} . Four bounding values are considered: $I_{c5} = 2.3, 2.4, 2.5$, and 2.6 . While it is often assumed that $I_c > 2.6$ delimits potentially liquefiable and non-liquefiable deposits, this value is likely conservative in the sense that $I_c = 2.6$ represents a high probability that the soil is not liquefiable rather than a definitive boundary, thus, bounding values < 2.6 are also assessed here. Additionally, soil profiles with $I_{c5} < 2.6$ can be comprised of significant proportions of soils deemed unlikely to liquefy. For example, the CPT logs with $I_{c5} \approx 2.4$ indicate that on average, such profiles have soils with $I_c \geq 2.6$ over more than 40% of the interval from 1.2 to 5 m depth.

5.2. Assessment of filtered V_{s5} models

Filtered V_{s5} models (called V_{s5f} for distinction purposes) are determined by removing all grid points with I_{c5} greater than each bounding value. The resulting V_{s5f} surfaces are shown successively in

Fig. 9 at the same scale, and over the same areal extents, as the liquefaction damage map of Fig. 8(a). The V_{s5f} surfaces do not correspond perfectly with liquefaction damage severity, however, they appear to work well in an overall sense. Certain areas correspond very well. For example, along the path of the Avon river (near region 6) the areas with the most severe surface manifestations of liquefaction correspond well with $V_{s5} < 95$ –100 m/s, while the areas of minor to moderate liquefaction correspond to higher V_{s5} values. The regions where these general observations tend to fail, such as the large area of low V_{s5} located south of the CBD (vicinity of region 4), tend to correspond to relatively high I_{c5} values (greater than about 2.2). Such locations may be places where the other factors that contribute to the uncertainty in liquefaction potential (e.g., soil age, plasticity, grain size distribution, fabric) reduce the probability of liquefaction susceptibility despite an I_{c5} value that may be classified as potentially liquefiable if considered alone. Such locations could also be places where the CPT- V_s correlation is tending to underpredict the soil V_s .

As the I_{c5} bounding value is decreased from 2.6 to 2.3, the overall correspondence between the V_{s5f} surfaces and the liquefaction damage map becomes more pronounced. This is likely due to the removal of zones where low V_{s5} values correspond to a higher concentration of soil types with a lower probability of liquefaction susceptibility, and surficial liquefaction manifestations were generally absent. The histograms accompanying each surface shown in Fig. 9 summarize the effect of reducing the I_{c5} filter value. These histograms were generated by identifying the liquefaction damage category (no damage, minor to moderate damage, severe damage) corresponding to each grid point in the V_{s5f} surfaces, and show the number of sites corresponding to each damage type and the distribution of these damage categories with V_{s5} magnitude. Based on these results, the V_{s5f} model shown in Fig. 9(a) with $I_{c5} < 2.6$ corresponds the worst with liquefaction damage. In this case, there is no discernible difference between the distributions of the three damage categories (the mean V_{s5} values are nominally identical) and the sites identified within the no damage category appear to be biased towards V_{s5} values that are too low. For each successive decrease in the I_{c5} filter, the V_{s5} values corresponding to each damage category become more distinct from each other, with no damage sites tending to be associated with higher V_{s5} and severe damage sites

remaining associated with lower V_{s5} .

Monte Carlo simulation is used to quantify how well the four V_{s5f} surfaces correspond with observations of liquefaction-related surficial damage. For the surface corresponding to each I_{c5} filter value, random V_{s5f} values are obtained from the empirical cumulative distribution functions for each damage category shown in Fig. 10 using the inverse transformation method. The random V_{s5f} values are compared to assess the distinction between two damage boundaries: the boundary between no damage and minor/moderate damage, and the boundary between minor/moderate and severe damage. This process is repeated 10,000 times for all four V_{s5f} surfaces to estimate the probabilities that the V_{s5f} values of the less severe liquefaction damage category for each damage boundary are greater than those for the corresponding more severe category. The results of these Monte Carlo simulations are summarized in Table 2. Overall, the boundary between minor/moderate and severe damage is captured well in the V_{s5f} models. There is a >50% probability that the minor/moderate grid points have a larger V_{s5f} than the severe damage points for all four I_{c5} filter values, and a significant probability for $I_{c5} < 2.4$ and 2.3. In contrast, the probabilities in Table 2 show that the boundary between no damage and minor/moderate damage is not well represented in the V_{s5f} models. Only the surfaces for $I_{c5} < 2.4$ and 2.3 show a >50% probability of higher V_{s5f} in the less severe damage category, and only $I_{c5} < 2.3$ shows a significant probability.

Based on the results presented here, the V_{s5f} models for $I_{c5} < 2.3$ and 2.4 correspond the best with the distinctions between the liquefaction damage categories. For these cases, there is a high probability that regions with lower values of V_{s5f} exhibited signs of more severe liquefaction-related damage following the 22 February 2011 earthquake, and the probability of damage severity decreases with increasing V_{s5f} . Based on Fig. 9, it appears that V_{s5f} less than 95–100 m/s correlates well with severe damage. It is more difficult to select a similarly definite bounding value to distinguish between the probability of minor/moderate damage and no damage, however, based on the empirical CDFs in Fig. 10, it appears that in areas with $V_{s5f} > 115$ m/s, it is more likely than not that no damage was observed.

The correlation between V_{s5f} and liquefaction damage is certainly not perfect, but there is a general trend that is revealed amongst the scatter as the I_{c5} filter is reduced. The correlation between observed liquefaction damage and liquefaction-related damage indices, such as LSN, reported in Figure 13 of van Ballegooy et al. [9] is similarly imperfect, also showing a significant amount of scatter for LSN-based prediction of liquefaction damage. It is hypothesized by van Ballegooy et al. [9] that among other potential sources, the widespread lateral spreading that comprises a major portion of the most severe liquefaction-related damage zones for the 22 February event likely accounts for

some of the observed scatter. Liquefaction-damage indices such as LSN and LPI are not intended to be reliable predictors of lateral spreading vulnerability, and therefore, may not provide an appropriate indication for such areas. Similarly, V_{s5f} does not provide any direct indication of vulnerability to lateral spreading, and may similarly misrepresent the severe damage zones where lateral spreading was observed. Another potential source of scatter in the correlation between V_{s5f} and liquefaction damage is related to the groundwater table. In the considered regions of Christchurch, the water table depth is generally within 1–2 m of the ground surface, however, this does not hold universally and the lack of information on the water table depth in filtered V_{s5} values may misrepresent the severity of the surface manifestation-induced consequences resulting from shallow liquefaction. It is also possible that underprediction of shear wave velocity from the CPT- V_s model concentrated in particular regions/locations, or some bias in the types of materials that were evaluated in the CPT dataset, could contribute to differences between V_{s5f} and observed liquefaction damage.

6. Conclusions

The effects of spatial variability in the near-surface soils of the greater Christchurch urban area were keenly evident in the ground motion records and damage observations associated with the 2010–2011 Canterbury earthquake sequence. A model of near-surface shear wave velocity developed using a Christchurch-specific CPT- V_s correlation [25,26] following the methodology described in the companion work of McGann et al. [1] was used to identify and characterize the spatial and depth variability of the near-surface soils of the region. Comparisons between V_{s30} and V_{sz} for $z < 30$ m showed that there is significant variability in V_s with depth across the Christchurch region, and that the degree of correlation between V_{s30} and V_{sz} differed based on the surficial geology of a given site. The degree of correlation between V_{s30} and V_{sz} for the considered Christchurch soils was also shown to differ with respect to similar correlations developed for sites in California, Japan, and Greece. The Christchurch data showed the greatest similarity to the Japan-based data, and it is likely that differences in depth to dense layers or bedrock were the primary source of differences between the considered relations.

The impact of this inherent V_s depth variability in the near-surface soils of the Christchurch region on expected seismic response was examined through the development of site classification maps following the NEHRP and NZS1170.5 classification schemes and through the computation of transfer functions for typical 30 m V_s profiles developed for the eight Christchurch subregions introduced in McGann et al. [1]. In terms of the considered site classification schemes, there is no great variation in general seismic response expected for different locations within the region. In contrast, the transfer functions determined for the typical 30 m profiles indicated that areas of nominally identical V_{s30} (and corresponding site class) may have local site effects in which higher amplification occurs in different modes and the modes occur at different frequencies. Comparisons to observations of the severity of liquefaction-induced damage made following the 22 February 2011 event were used to assess the degree of correspondence between the regional V_{s5} model and the observed liquefaction. It was shown that when filtered based on the 5 m average soil behaviour type index (I_{c5}), the V_{s5} model corresponds well in a general sense, with areas of severe liquefaction damage characterized by lower V_{s5} values, and areas of little or no damage characterized by higher V_{s5} values or higher I_{c5} values that indicate less likelihood for a prevalence of liquefaction-susceptible soil types in the upper 5 m zone.

Acknowledgments

Funding for this work was provided by the Rutherford Discovery Fellowship (RSNZ), the New Zealand Earthquake Commission (EQC), and the New Zealand Natural Hazards Research Platform (NHRP). The

Table 2
Probabilities of greater V_{s5} in the less severe damage category for four I_{c5} filter values and two damage boundaries.

Damage boundary	$I_{c5} < 2.6$	$I_{c5} < 2.5$	$I_{c5} < 2.4$	$I_{c5} < 2.3$
No damage to minor/mod. damage	18%	23%	62%	90%
Minor/mod. damage to severe damage	67%	71%	86%	99%

authors would also like to thank the Canterbury Geotechnical Database team for providing access to data used in this study.

Appendix A. NEHRP and NZS1170.5:2004 site classification systems

A brief summary of the NZS1170.5 and NEHRP site classification systems is provided here for reference. Further and more detailed information can be found in [12,13,15].

A.1. NZS1170.5:2004 site classification

Site classification in the New Zealand standard, NZS1170.5 [15], is defined in terms of several properties, including: V_{s30} ; the small-strain (low-amplitude in [15]) site period T_{soil} (computed as four times the shear wave travel time from surface to rock); the unconfined compressive strength q_u , the undrained shear strength s_u , SPT N-value, and V_s . There are five discrete site classes A, B, C, D, and E. The criteria and description of each class are summarized in Tables 3, 4.

Table 3

Site classes per NZS1170.5 [15].

Class	Description	V_{s30} (m/s)	V_s (m/s)	q_u (MPa)	T_{soil} (s)	s_u (MPa)	SPT N	Notes
A	Strong rock	>1500	–	>50	–	–	–	[1]
B	Rock	360 to 1500	–	1 to 50	–	–	–	[2]
C	Shallow soil	–	–	–	≤0.6	–	–	[3]
D	Deep/soft soil	–	–	–	>0.6	<12.5 ^[4]	<6 ^[4]	[5]
E	Very soft soil	–	≤150 ^[6]	–	–	<12.5 ^[6]	<6 ^[6]	–

[1] Profile not underlain by materials with $q_u < 18$ MPa or $V_s < 600$ m/s.

[2] Profile not underlain by materials with $q_u < 0.8$ MPa or $V_s < 300$ m/s.

[3] Not class A, B, or E. Meets depth requirements of Table 4.

[4] Underlain by <10 m of soils with these values.

[5] Not class A, B, or E. Meets depth requirements of Table 4.

[6] Site with >10 m of soils with any of these values, or >10 m combined depth of soils with all three properties.

Table 4

Depth limits for NZS1170.5:2004 [15] Class C and D.

Cohesive soils		Cohesionless soils	
s_u (kPa)	Max depth of soil (m)	SPT N	Max depth of soil (m)
<12.5	0	<6	0
12.5 to 25	20	6 to 10	40
25 to 50	25	10 to 30	45
50 to 100	40	30 to 50	55
100 to 200	60	>50	60

Table 5

V_{s30} -based site classes per NEHRP [12,13].

Class	Description	V_{s30} (m/s)
A	Hard rock	>1500
B	Rock	760 to 1500
C	Very dense soil/soft rock	360 to 760
D	Stiff soil	180 to 360
E	Soft soil	<180
F	Special soils	

A.2. NEHRP site classification

In the United States, the NEHRP [12,13] site classes are primarily based on V_{s30} alone. There are six classes A, B, C, D, E, and F. The V_{s30} extents for these classes are as summarized in Table 5. Site class F is a special category for potentially problematic soils that require a site-specific evaluation.

References

- [1] McGann CR, Bradley BA, Cubrinovski M. Development of regional V_{s30} model and typical V_s profiles for Christchurch, New Zealand from CPT data and region-specific CPT- V_s correlation. *Soil Dyn Earthq Eng* 2016, [under review].
- [2] Bradley BA, Cubrinovski M. Near-source strong ground motions observed in the 22 February 2011 Christchurch earthquake. *Seismol Res Lett* 2011;82(6):853–65.
- [3] Bradley BA. Strong ground motion characteristics observed in the 4 September 2010 Darfield, New Zealand earthquake. *Soil Dyn Earthq Eng* 2012;42:32–46.
- [4] Cubrinovski M, Green RA, Allen J, Ashford SA, Bowman E, Bradley BA, et al. Geotechnical reconnaissance of the 2010 Darfield (Canterbury) earthquake. *Bull NZ Soc Earthq Eng* 2010;43(4):243–320.
- [5] GEER. Geotechnical Reconnaissance of the 2010 Darfield (New Zealand) Earthquake. Geo-Engineering Extreme Events Reconnaissance (GEER) Association. Green RA, Cubrinovski M, editors. Report No. GEER-024; 2010.
- [6] Cubrinovski M, Bradley BA, Wotherspoon LM, Green RA, Bray JD, Wood C, et al. Geotechnical aspects of the 22 February 2011 Christchurch earthquake. *Bull NZ Soc Earthq Eng* 2011;44(4):205–26.
- [7] Cubrinovski M, Bray JD, Taylor ML, Giorgini S, Bradley BA, Wotherspoon LM, et al. Soil liquefaction effects in the central business district during the February 2011 Christchurch earthquake. *Seismol Res Lett* 2011;82(6):893–904.
- [8] GEER. Geotechnical Reconnaissance of the 2011 Christchurch, New Zealand Earthquake. Geo-Engineering Extreme Events Reconnaissance (GEER) Association; 2011. Cubrinovski M, Green RA, Wotherspoon L, editors. Report No. GEER-027.
- [9] van Ballegooy S, Malan P, Lacrosse V, Jacka ME, Cubrinovski M, Bray JD, et al. Assessment of liquefaction-induced land damage for residential Christchurch. *Earthq Spectra* 2014;30(1):31–55.
- [10] Bradley BA. Ground motions observed in the Darfield and Christchurch earthquakes and the importance of local site response effects. *NZ J Geol Geophys* 2012;55(3):279–86.
- [11] Bradley BA. Systematic ground motion observations in the Canterbury earthquakes and region-specific non-ergodic empirical ground motion modeling. *Earthq Spectra* 2015. <http://dx.doi.org/10.1193/053013epa137m>, [in press].
- [12] Building Seismic Safety Council. NEHRP Recommended provisions for seismic regulations for new buildings and other structures, Part I: provisions. Report No. FEMA-450. Federal Emergency Management Agency, Washington, D.C.; 2003.
- [13] American Society of Civil Engineers. Minimum design loads for buildings and other structures (7-10, third printing). Standards ASCE/SEI 7-10; 2013.
- [14] Eurocode 8. Design of structures for earthquake resistance, Part 1: general rules, seismic actions and rules for buildings. EN 1998-1. European Committee of Standardization (CEN); 2004.
- [15] Standards New Zealand. Structural design actions Part 5: earthquake actions – New Zealand. NZS1170.5; 2004.
- [16] Boore DM. Estimating V_{s30} (or NEHRP site classes) from shallow velocity models (depths <30 m). *Bulletin of the Seismological Society of America* 2004;94(2):591–7.
- [17] Boore DM, Thompson EM, Cadet H. Regional correlations of V_{s30} and velocities averaged over depths less than and greater than 30 meters. *Bulletin of the Seismological Society of America* 2011;101(6):3046–59.
- [18] Stewart JP, Klimis N, Savvaidis A, Theodoulidis N, Zargli E, Athanasopoulos G, et al. Compilation of a local V_s profile database and its application for inference of V_{s30} from geologic- and terrain-based proxies. *Bulletin of the Seismological Society of America* 2014;104(6):2827–41.
- [19] McGann CR, Bradley BA, Cubrinovski M. High-Density Shallow Shear Wave Velocity Characterisation of the Urban Christchurch, New Zealand Region. University of Canterbury Research Report No. 2015-02; 2015.
- [20] Brown LJ, Weeber JH. *Geology of the Christchurch urban area*. Lower Hutt, New Zealand: Institute of Geological and Nuclear Sciences Ltd.; 1992.
- [21] Lee RL, Bradley BA, Pettinga JR, Hughes MW, Graves RW. Ongoing development of a 3D seismic velocity model of Canterbury, New Zealand for broadband ground motion simulation. in: New Zealand Society for earthquake engineering annual technical conference. Auckland. 21–23 March, Paper No. 8; 2014.
- [22] Okada Y, Kasahara K, Hori S, Obara K, Sekiguchi S, Fujiwara H, et al. Recent progress of seismic observation networks in Japan – Hi-net, F-net, K-NET and KiK-net. *Earth Planets Space* 2004;56:xv–xxviii.
- [23] McGann CR, Bradley BA. Ongoing development of a near-surface shear wave velocity (V_s) model for Christchurch using a region-specific CPT- V_s correlation. In: Proceedings of the 12th Australia New Zealand conference on geomechanics (ANZ 2015). February 22–25. Wellington, New Zealand; 2015.
- [24] Wilson J. Christchurch swamp to city. A short history of the Christchurch Drainage Board 1875–1989. Lincoln: Te Waihora Press; 1989.
- [25] McGann CR, Bradley BA, Taylor ML, Wotherspoon LM, Cubrinovski M. Applicability of existing empirical shear wave velocity correlations to seismic cone penetration test data in Christchurch New Zealand. *Soil Dyn Earthq Eng* 2015;75:76–86. <http://dx.doi.org/10.1016/j.soildyn.2015.03.021>.
- [26] McGann CR, Bradley BA, Taylor ML, Wotherspoon LM, Cubrinovski M. Development of an empirical correlation for predicting shear wave velocity of Christchurch soils from cone penetration test data. *Soil Dyn Earthq Eng* 2015;75:66–75. <http://dx.doi.org/10.1016/j.soildyn.2015.03.023>.
- [27] Wotherspoon LM, Bradley BA, Thomson EM, Hills AJ, Jeong S, Wood CM, et al. Development of deep V_s profiles and site periods for the Canterbury region. in: New Zealand Society for Earthquake Engineering Annual Conference. Rotarua, April 10–12. Paper No. O-59; 2015, p. 537–44.
- [28] Lee RL, Bradley BA, Ghisetti FC, Pettinga JR, Hughes MW, Thomson EM. A geology-based 3D seismic velocity model of Canterbury, New Zealand. in: New Zealand Society for earthquake engineering annual technical conference. Rotarua, 10–12 April, Paper No. O-63; 2015. p. 570–7.
- [29] Information Services Christchurch City Council. Christchurch area showing waterways swamps & \$2 vegetation cover in 1856. (<http://resources.ccc.govt.nz/files/blackmap-environmentecology.pdf>); 2006 [accessed 26.08.14].
- [30] Robertson PK, (Fear) Wride CE. Evaluating cyclic liquefaction potential using the cone penetration test. *Can Geotech J* 1998;35(3):442–59.